Journal of Porphyrins and Phthalocyanines
J. Porphyrins Phthalocyanines 2018; **22**: 461–468
DOI: 10.1142/S1088424618500906

Published at http://www.worldscinet.com/jpp/

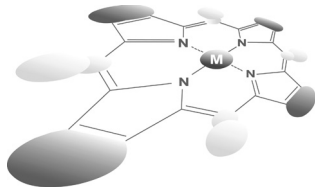

Vibrational structure analysis of cobalt fluoro-porphyrin surface coatings on gallium phosphide

Diana Khusnutdinova, Anna M. Beiler, Brian L. Wadsworth, Sylvia K. Nanyangwe and Gary F. Moore*◊

School of Molecular Sciences and the Biodesign Institute Center for Applied Structural Discovery (CASD), Arizona State University, Tempe, AZ 85287-1604, USA

Received 19 April 2018
Accepted 1 June 2018

ABSTRACT: Grazing angle attenuated total reflectance Fourier transform infrared (GATR–FTIR) spectroscopy is used to characterize chemically modified gallium phosphide (GaP) surfaces containing grafted cobalt(II) porphyrins with 3-fluorophenyl substituents installed at the *meso*-positions. In these hybrid constructs, porphyrin surface attachment is achieved using either a two-step method involving coordination of cobalt fluoro-porphyrin metal centers to nitrogen sites on an initially applied thin-film polypyridyl surface coating, or *via* a direct modification strategy using a cobalt fluoro-porphyrin precursor bearing a covalently bonded 4-vinylphenyl surface attachment group at a β-position. Both surface-attachment chemistries leverage the UV-induced immobilization of alkenes but result in distinct structural connectivities of the grafted porphyrin units and their associated vibrational spectra. In particular, the in-plane deformation vibrational frequency of metalloporphyrin components in samples prepared *via* coordination to the polymeric interface is characterized by an eight wavenumber shift to higher frequencies compared to that measured on metalloporphyrin-modified surfaces prepared using the one-step attachment method. The more rigid ring structure in the polymeric architecture is consistent with coordination of porphyrin cobalt centers to pyridyl-nitrogen sites on the surface graft. These results demonstrate the use of GATR–FTIR spectroscopy as a sensitive tool for characterizing porphyrin-modified surfaces with absorption signals that are close to the detection limits of many common spectroscopic techniques.

KEYWORDS: porphyrins, semiconductors, gallium phosphide, catalysis, surface chemistry, grazing angle infrared spectroscopy.

INTRODUCTION

Molecular-modified surfaces have applications in a range of existing and emerging technologies [1–4]. In the context of chemical catalysis, supported molecular assemblies offer a promising approach to combining favorable features associated with homogeneous catalysts, including enhanced synthetic control over their physical properties as dictated by their well-defined structures, with those of heterogeneous catalysts, where solid-state form factors can be more conducive to industrial applications but the reactive site structures are inherently less well-defined and often more difficult to manage. In addition, the use of solid-state electrodes as a support provides a means for activating immobilized redox catalysts at electrified interfaces.

Such hybrid materials have been reported using a range of chemical approaches to assemble molecular components onto conducting or semiconducting substrates [5–10]. In these constructs, chemical transformations can be triggered by application of an electrochemical bias or, in the case of photochemically active materials, by illumination of the sample. While fundamentally interesting, practical applications of such technologies demand improved understanding and control over the structural properties governing the function of these architectures.

◊ SPP full member in good standing

*Correspondence to: Gary F. Moore, email: gfmoore@asu.edu.

In this report, we highlight the use of grazing angle attenuated total reflectance Fourier transform infrared (GATR–FTIR) spectroscopy as a non-destructive and surface-sensitive characterization technique capable of identifying organic and inorganic species, including surface functional groups, on substrates with relatively high refractive indexes [11–13]. The amplification of signal achieved *via* GATR–FTIR spectroscopy is due to the grazing angle conditions and resulting enhanced electric field. However, quantitative analysis of surface composition based on absolute FTIR signal intensities, which are sensitive to the pressure of contact between the substrate and sample mount, is limited to relative peak intensity analysis [14, 15].

This current study focuses specifically on structural characterization of cobalt fluoro-porphyrin-modified surfaces of gallium phosphide. The metalloporphyrin components used in this work belong to a group of tetrapyrrolic molecules that serve important roles as enzymatic reactive sites in biological processes and as components in molecular-based materials with technological applications, including catalysis [16–29]. In particular, cobalt fluoro-porphyrins have been shown to serve as homogeneous electrocatalysts for hydrogen evolution and carbon dioxide reduction when dissolved in solutions containing the appropriate substrates [30, 31]. By contrast, gallium phosphide belongs to the III–V class of semiconductors, is used as a light-emitting diode in industrial applications, and functions as a light capture and conversion component in emerging technologies with applications in photoelectrosynthetic fuel production [32–36].

The molecular surface coatings used in this report are composed of cobalt fluoro-porphyrin units immobilized onto gallium phosphide (GaP) substrates *via* two different methods. The first approach relies on immobilization of cobalt(II) 5,10,15,20-tetrakis(3-fluorophenyl)porphyrin (**1**) to a sample of GaP containing an initially applied thin-film polypyridyl coating, **PVP|GaP**, yielding samples of **CoT3FPP|PVP|GaP** (Scheme 1, top). In this method, pyridyl-nitrogen sites on the **PVP|GaP** surface serve as molecular recognition units to self-assemble cobalt porphyrins along the polymeric interface. The second preparation method involves direct application of a cobalt fluoro-porphyrin complex bearing a 4-vinylphenyl surface attachment group covalently attached at a β-position on the macrocycle. Treatment of unmodified-GaP surfaces, **GaP**, with solutions of this precursor, cobalt(II) 5,10,15,20-tetrakis(3-fluorophenyl)-2-(4-vinylphenyl) porphyrin (**2**), in the presence of UV light yields samples of **CoT3FPP|GaP** (Scheme 1, bottom). The surfaces of these two constructs, **CoT3FPP|PVP|GaP** and **CoT3FPP|GaP**, possess distinct IR vibrational modes in the range of 980–1740 cm^{-1}, allowing structural analysis and comparison of the cobalt fluoro-porphyrin components in these hybrid architectures.

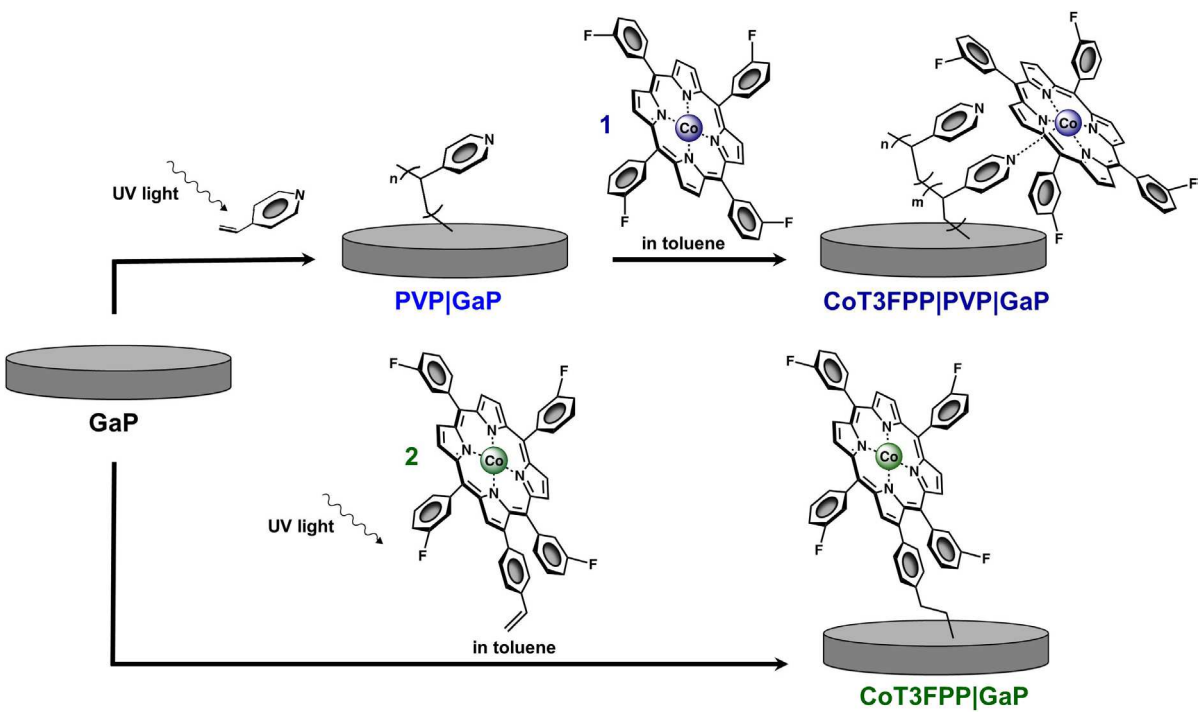

Scheme 1. Schematic representation depicting the attachment methods, materials, and reagents used to prepare cobalt fluoro-porphyrin surface coatings on gallium phosphide (see main text for details)

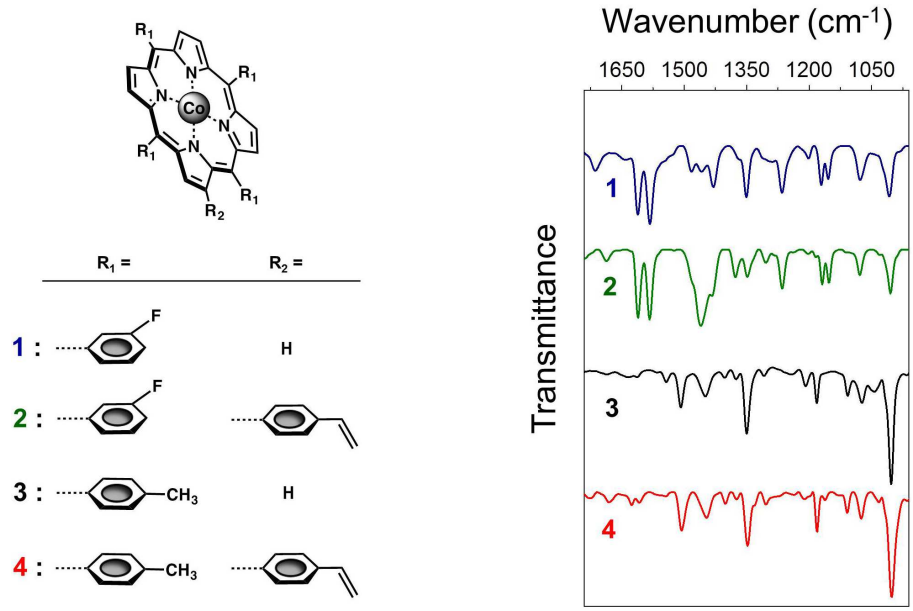

Fig. 1. (Left panel) Molecular structures of the fluorinated and non-fluorinated model compounds and precursors, including cobalt(II) 5,10,15,20-tetrakis(3-fluorophenyl)porphyrin (**1**), cobalt(II) 5,10,15,20-tetrakis(3-fluorophenyl)-2-(4-vinylphenyl) porphyrin (**2**), cobalt(II) 5,10,15,20-tetra-*p*-tolylporphyrin (**3**), and cobalt(II) 5,10,15,20-tetra-*p*-tolyl-2-(4-vinylphenyl)porphyrin (**4**) used to assemble **CoT3FPP|PVP|GaP**, **CoT3FPP|GaP**, **CoTTP|PVP|GaP**, and **CoTTP|GaP**, respectively. (Right panel) FTIR transmission spectra of **1** (dark blue), **2** (green), **3** (black), and **4** (red) collected in KBr

RESULTS AND DISCUSSION

Materials preparation

All reagents were purchased from Sigma-Aldrich. Dichloromethane, methanol, and toluene were freshly distilled before use. All semiconductors were purchased from University Wafers. The porphyrins used in this work, including cobalt(II) 5,10,15,20-tetrakis(3-fluorophenyl) porphyrin (**1**), cobalt(II) 5,10,15,20-tetrakis(3-fluorophenyl)-2-(4-vinylphenyl)porphyrin (**2**), cobalt(II) 5,10,15,20-tetra-*p*-tolylporphyrin (**3**), and cobalt(II) 5,10,15,20-tetra-*p*-tolyl-2-(4-vinylphenyl)porphyrin (**4**) (Fig. 1) were prepared following previously reported methods [37–39].

Samples of **GaP** were chemically modified using an adaptation of previously reported procedures (see experimental section for details) [40–45]. In short, **GaP** wafers were chemically etched with hydrofluoric acid and then immersed into argon-sparged solutions of neat 4-vinylpyridine or 1 mM cobalt(II) 5,10,15,20-tetrakis(3-fluorophenyl)-2-(4-vinylphenyl)porphyrin (**2**) in toluene, followed by 2 h of illumination under shortwave UV light (254 nm), yielding samples of **PVP|GaP** or **CoT3FPP|GaP**, respectively. The **PVP|GaP** wafers were then further modified in a second wet-chemical treatment step involving exposure to 1 mM cobalt(II) 5,10,15,20-tetrakis(3-fluorophenyl)porphyrin (**1**) in toluene for 12 h to yield samples of **CoT3FPP|PVP|GaP** (Scheme 1). These surface modification strategies leverage the UV-induced grafting chemistry of olefins to hydroxyl and oxygen-terminated surfaces [46–49]. Modified substrates at each step of surface preparation and functionalization were characterized using X-ray photoelectron (XP) as well as GATR–FTIR spectroscopies.

Structural characterization

FTIR transmission spectra of the cobalt fluoro-porphyrin molecules used in this work (**1** and **2**) were collected in a matrix of KBr and are shown in Fig. 1 (blue and green lines, respectively). For comparison, spectra of model non-F-containing cobalt porphyrins (**3** and **4**) are also included in Fig. 1 (black and red lines, respectively). All four spectra contain similar vibrational features associated with the core porphyrin macrocycles, including bands that can be assigned to

Table 1. In-plane cobalt porphyrin deformation frequencies measured using samples composed of **1**, **2**, **3**, or **4** in KBr

ν_{Co-N} of the molecular precursors	
Precursor	ν_{Co-N} (cm^{-1})
1	1007
2*	1005
3*	1003
4*	1001

* values have been previously reported [37, 38, 42].

C_β–H (1170–1078 cm^{-1}), C_m–C_{ph} (1265 cm^{-1}), C_α–N and C_α–C_β (1350–1369 cm^{-1}), as well as C_β–C_β, C_α–C_m, and C=C (1430–1612 cm^{-1}) vibrations [50–58]. We note the conjugated ring structure of these complexes likely gives rise to a high degree of vibrational coupling between the various metalloporphyrin modes, thus complicating descriptions of their normal modes. Nonetheless, unlike the transmission spectra of **3** and **4**, the spectra of **1** and **2** include strong IR absorption bands located between 1133–1178 cm^{-1} and 1554–1627 cm^{-1} associated with C–F bond vibrations of the 3-fluorophenyl substituents [59–62]. Further differences between these four spectra include the vibrational frequency of a metal-sensitive band ascribed to an in-plane cobalt porphyrin deformation, $\nu_{Co–N}$ (where ν is the vibrational frequency). For samples **1** and **3**, this mode is observed at 1007 cm^{-1} or 1003 cm^{-1}, respectively (Table 1). In these examples, the 3-fluorophenyl groups at the *meso*-positions of **1** perturb the $\nu_{Co–N}$, offsetting it to higher values compared to those measured using samples of the non-fluorinated cobalt porphyrin analog, **3**. A similar offset ($\Delta\nu_{Co–N}$) is observed when comparing the $\nu_{Co–N}$ values measured using samples of the fluorinated and non-fluorinated 4-vinylphenyl containing precursors **2** and **4** (Table 1). However, for these compounds (**2** and **4**) the in-plane cobalt porphyrin deformation vibrational modes appear at slightly lower frequencies compared to the corresponding values measured using samples of **1** and **3**, where a proton appears in place of the 4-vinylphenyl surface attachment moiety.

The GATR–FTIR absorption spectrum of an HF-etched **GaP** surface is included in Fig. 2b (black), showing characteristic broad in energy oxide-related absorption bands assigned to OH and PO_x^- surface functional groups [50], centered at 1680 and 1200 cm^{-1}, as well as a band at 1440 cm^{-1} associated with the presence of adventitious carbon (CH_x). Conversely, GATR–FTIR spectra of **PVP|GaP** surfaces are characterized by relatively strong absorption features appearing from 1400–1600 cm^{-1} that are assigned to C–N, C=N, C–H, and CH_2 vibrations of the surface-attached polypyridyl chains (Fig. 2b, blue), confirming successful attachment of the polymeric surface coating, and consistent with previous reports [40–43]. The mode appearing at 1453 cm^{-1} is particularly diagnostic of the planar deformation vibration of CH_2 groups in polymeric chains. For example, this mode is observed in samples of polyvinylpyridine and polystyrene but is not present in spectra of 4-vinylpyridine and styrene monomers [63].

GATR–FTIR absorption spectra of **CoT3FPP|PVP|GaP** surfaces (Fig. 2b, dark blue) show several vibrational features associated with the presence of cobalt fluoro-porphyrin species, including modes associated with C_β–H (1068–1174 cm^{-1}), C_m–C_{ph} (1263 cm^{-1}), C_α–N and C_α–C_β (1310–1378 cm^{-1}), as well as C_β–C_β, C_α–C_m, and C=C

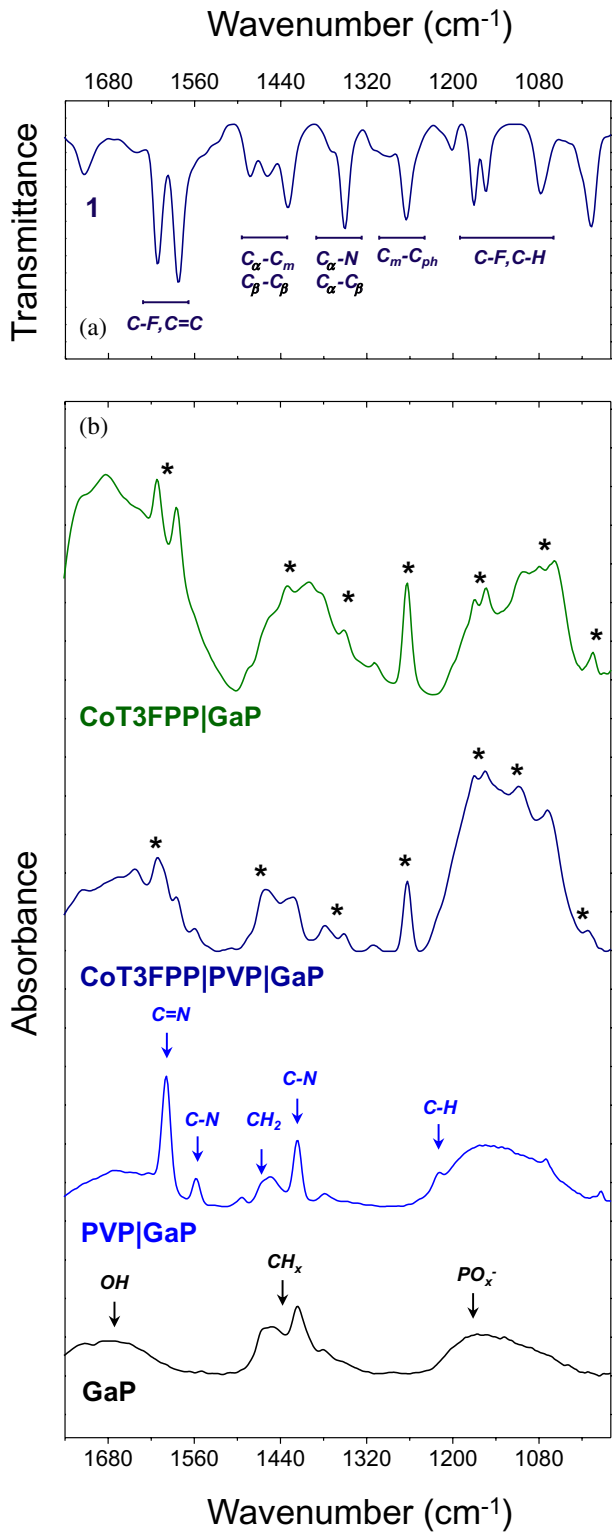

Fig. 2. (a) FTIR transmission spectrum of **1** collected in KBr, included to facilitate comparisons, as well as (b) GATR–FTIR absorption spectra collected using samples of **GaP** (black), **PVP|GaP** (blue), **CoT3FPP|PVP|GaP** (dark blue), and **CoT3FPP|GaP** (green). Surface vibrational modes associated with immobilized cobalt fluoro-porphyrin species are labeled with *

Table 2. In-plane cobalt porphyrin deformation frequencies measured on surfaces of **CoT3FPP|PVP|GaP**, **CoT3FPP|GaP**, **CoTPP|PVP|GaP**, and **CoTPP|GaP**

ν_{Co-N} on molecular modified surfaces	
Construct	ν_{Co-N} (cm^{-1})
CoT3FPP|PVP|GaP	1012
CoT3FPP|GaP	1005
CoTTP|PVP|GaP*	1009
CoTTP|GaP*	1001

* values have been previously reported [38, 42].

(1508–1643 cm^{-1}) vibrations that appear at values nearly identical to those recorded using samples of the associated molecular precursor **1** in KBr. In addition, several absorption features appearing in the 1400–1600 cm^{-1} region on surfaces of **CoT3FPP|PVP|GaP** are assigned to vibrational modes associated with polypyridyl units. However, contributions associated with porphyrin ring-based modes also appear in this spectral region, complicating a detailed analysis and assignment of all features. Nonetheless, the in-plane metalloporphyrin deformation vibrational modes, appearing between 1000–1019 cm^{-1}, are exquisitely sensitive to both the elemental nature of the metal center and its local coordination environment [64–67]. Thus, they are also sensitive to the nature of the chemical attachment strategies used in this report to assemble cobalt fluoro-porphyrin-modified GaP surfaces.

As previously reported for chemically modified surfaces composed of non-fluorinated cobalt porphyrin, **3**, assembled onto polypyridyl functionalized gallium phosphide substrates, forming **CoTTP|PVP|GaP** [42], attachment of porphyrin cobalt centers to surface-grafted pyridyl-nitrogen sites results in a change of the porphyrin's original four-coordinate square planar environment and a diagnostic shift of the in-plane cobalt porphyrin deformation vibration to higher frequencies ($\Delta\nu_{Co-N}$ ~ 6 cm^{-1}). For the F-containing cobalt porphyrins described in this report, coordination to the surface-grafted pyridyl units gives rise to a similar offset ($\Delta\nu_{Co-N}$ ~ 6 cm^{-1}) of the vibrational frequencies associated with the cobalt fluoro-porphyrin deformation modes (Tables 1 and 2). In addition, features arising from C–F bond vibrations are observed at 1155–1171 cm^{-1} and 1585–1643 cm^{-1} on **CoT3FPP|PVP|GaP** samples, providing further evidence of successful intact fluoro-porphyrin incorporation on these surfaces.

GATR–FTIR analysis of **CoT3FPP|GaP** samples, prepared using the direct attachment method, also shows the presence of surface vibrational modes characteristic of cobalt fluoro-porphyrins, including those with frequencies ascribed to C_β–H (1059–1080 cm^{-1}), C_m–C_{ph} (1263 cm^{-1}), C_α–N and C_α–C_β (1309–1400 cm^{-1}), C_β–C_β, C_α–C_m, C=C (1431–1612 cm^{-1}), and C–F (1153–1167 cm^{-1} and 1585 cm^{-1}) vibrations (Fig. 2b, green). Yet as anticipated, the ν_{Co-N} measured on surfaces of **CoT3FPP|GaP** samples appears at 1005 cm^{-1}, a value that is unperturbed compared to the ν_{Co-N} measured using samples of the non-surface immobilized fluoro-porphyrin precursor complex, **2**, and eight wavenumbers lower in frequency than those measured on surfaces of **CoT3FPP|PVP|GaP** (Fig. 3).

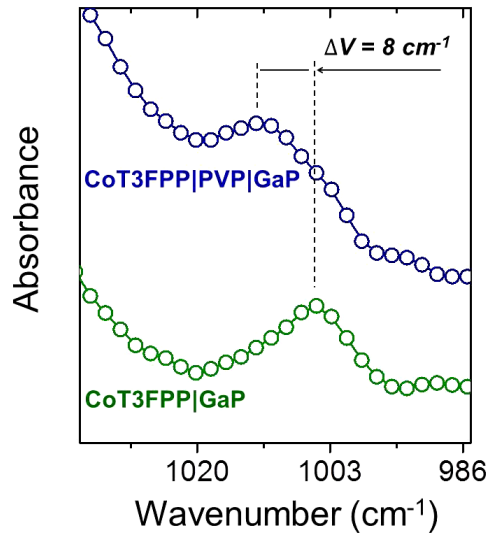

Fig. 3. GATR–FTIR absorption spectra of **CoT3FPP|GaP** (green) and **CoT3FPP|PVP|GaP** (dark blue) samples showing an eight wavenumber difference in vibrational frequency of the in-plane metalloporphyrin deformation mode

This similarity of the in-plane cobalt porphyrin deformation vibrational frequencies measured on surfaces of **CoT3FPP|GaP** and samples of **2** is consistent with previous reports [38] describing a non-fluorinated cobalt porphyrin-modified construct **CoTTP|GaP**, where the ν_{Co-N} is observed at 1001 cm^{-1} on surfaces of these samples and is identical to the ν_{Co-N} measured using samples of the non-fluorinated cobalt porphyrin precursor, **4**. For the fluorinated porphyrin samples **1** and **2**, the relatively higher frequency in-plane metalloporphyrin deformations compared to those measured using samples of the non-fluorinated complexes **3** or **4** (Table 1), indicate a more rigid ring structure for the F-containing congeners.

In addition to the structural information provided by IR-spectral analysis of the cobalt fluoro-porphyrin-modified GaP constructs **CoT3FPP|GaP** and **CoT3FPP|PVP|GaP**, XP spectroscopy confirms the presence of cobalt species on the surface and provides further information on the oxidation state of the metal centers (Fig. 4). In particular, high-energy resolution Co $2p_{3/2}$ core level spectra of **CoT3FPP|GaP** and **CoT3FPP|PVP|GaP** samples show a single peak centered at 781.2 eV and 781.0 eV, respectively, with a satellite feature at higher binding energies. These results

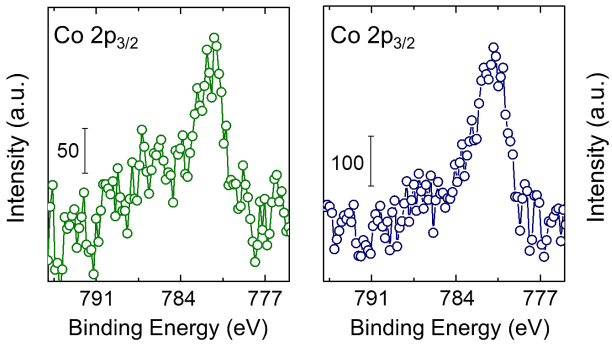

Fig. 4. High-energy resolution core level XP spectra of the Co $2p_{3/2}$ region recorded using samples of **CoT3FPP|GaP** (green) and **CoT3FPP|PVP|GaP** (dark blue)

are consistent with the presence of surface-immobilized cobalt species that are predominately in a 2 + oxidation state [68–71].

CONCLUSIONS

Hybrid materials consisting of gallium phosphide semiconductors chemically modified with cobalt fluoro-porphyrins were prepared *via* two methods: (1) coordination of fluoro-porphyrin cobalt centers to an initially applied polymeric interface and (2) direct attachment of cobalt fluoro-porphyrins containing covalently attached 4-vinylphenyl functional groups. Structural analysis of the resulting constructs using GATR–FTIR and XP spectroscopies confirms the presence of intact cobalt fluoro-porphyrin species on these surfaces. In addition, FTIR analysis provides a technique for measuring in-plane metalloporphyrin deformation vibrational frequencies, which can be used as a diagnostic spectroscopic handle for characterizing the binding environments of surface-immobilized porphyrins. In particular the frequency of the in-plane cobalt porphyrin deformation vibration measured on surfaces of **CoT3FPP|PVP|GaP** is eight wavenumbers higher than that measured on surfaces of **CoT3FPP|GaP**, indicating a more rigid ring structure in these assemblies that is consistent with coordination of cobalt porphyrin metallocenters to pyridyl-nitrogen sites on the PVP surface coating. The concepts described here highlight the sensitivity and non-destructive nature of GATR–FTIR as a tool for analyzing thin-film surface coatings and grafted molecular species, providing spectroscopic information that is not typically obtainable using more traditional infrared-based techniques.

EXPERIMENTAL

GaP*(100) *wafers. The semiconductor supports used in this work are single crystalline *p*-type Zn-doped gallium phosphide (100) wafers that are single side polished to an epi-ready finish. The wafers have a resistivity of 0.16 $\Omega \cdot$cm, a mobility of 69 $cm^2 \cdot V^{-1} \cdot s^{-1}$, and a carrier concentration of 4.5×10^{17} cm^{-3}, with an etch pit density of less than 5×10^4 cm^{-2}.

Sample preparation. Diced gallium phosphide samples were etched with buffered hydrofluoric acid and dried under nitrogen prior to wet chemical treatment with an argon-sparged solution of the neat monomer 4-vinylpyridine or 1 mM of **2** under UV light (254 nm) for 2 h. The samples were rinsed with methanol and dried under argon to yield samples of **PVP|GaP** and **CoT3FPP|GaP**, respectively. **PVP|GaP** samples were exposed to a 1 mM solution of **1** in toluene for 12 h to yield **CoT3FPP|PVP|GaP** samples that were rinsed with toluene and dried under nitrogen.

FTIR. Grazing angle attenuated total reflection Fourier transform infrared (GATR–FTIR) spectroscopy was performed using a VariGATR accessory (Harrick Scientific) with a Ge crystal plate installed in a Bruker Vertex 70. A minimum of 2 individual wafers were tested for each sample. Samples were pressed against the Ge crystal to ensure effective optical coupling. Spectra (256 scans) were collected under a dry nitrogen purge with a 4 cm^{-1} resolution, GloBar MIR source, a broadband KBr beamsplitter, and a liquid nitrogen-cooled MCT detector. Background measurements (256 scans) were obtained from the bare Ge crystal and the data were processed using OPUS software. GATR–FTIR measurements were baseline corrected for rubberband scattering. Spectra of model compounds in pressed KBr pellets were acquired with the same settings but using transmission mode.

XPS. X-ray photoelectron (XP) spectroscopy was performed using a monochromatized Al Kα source (hν = 1486.6 eV), operated at 63 W, on a Kratos system at a takeoff angle of 0° relative to the surface normal and a pass energy for narrow scan spectra of 20 eV at an instrument resolution of approximately 700 meV. A minimum of 2 wafers were analyzed for each sample. Survey spectra (40 scans) were collected with a pass energy of 150 eV. Spectral fitting was performed using Casa XPS analysis software and all spectra were calibrated by adjusting the C 1s core level position to 284.8 eV.

Acknowledgments

This material is based upon work supported by the National Science Foundation under Early Career Award 1653982. B.L.W. and A.M.B. were supported by an IGERT–SUN fellowship funded by the National Science Foundation (1144616). A.M.B received additional support from the Phoenix Chapter of the ARCS Foundation and the P.E.O Scholar Award. D.K. acknowledges support from ASU LightWorks under the Technology and Research Initiative Funds. The authors gratefully acknowledge Timothy Karcher in the LeRoy Eyring Center for Solid State Science for assistance with XPS data collection.

REFERENCES

1. Gooding JJ and Ciampi S. *Chem. Soc. Rev*. 2011; **40**: 2704–2718.
2. Vilan A and Cahen D. *Chem. Rev.* 2017; **117**: 4624–4666.
3. Basic Research Needs for Catalysis Science to Transform Energy Technologies. U.S. Department of Energy: Basic Energy Science Workshop Report. U.S. Government Printing Office: Washington, DC, 2017.
4. Forbes MDE. *ACS Cent. Sci.* 2015; **1**: 354–363.
5. Wang M, Yang Y, Shen J, Jiang J and Sun L. *Sustainable Energy Fuels* 2017; **1**: 1641–1663.
6. Queyriaux N, Kaeffer N, Morozan A, Chavarot-Kerlidou M and Artero V. *Journal Photochem. Photobiol., C* 2015; **25**: 90–105.
7. Wen F and Li C. *Acc. Chem. Res.* 2013; **46**: 2355–2364.
8. Bullock RM, Das AK and Appel AM. *Chem. —Eur. J.* 2017; **23**: 7626–7641.
9. Jiao J, Yu M, Holten D, Lindsey JS and Bocian DF. *J. Porphyrins Phthalocyanines* 2017; **21**: 453–464.
10. McKone JR, Marinescu SC, Brunschwig BS, Winkler JR and Gray HB. *Chem. Sci.* 2014; **5**: 865–878.
11. Milosevic M, Milosevic V and Berets SL. *Appl. Spectrosc.* 2007; **61**: 530–536.
12. Milosevic M. *Applied Spectrosc. Rev.* 2004; **39**: 365–384.
13. Mulcahy ME, Berets SL, Milosevic M and Michl J. *J. Phys. Chem. B* 2004; **108**: 1529–1521.
14. O'Leary LE, Johansson E, Brunschwig BS and Lewis NS. *J. Phys. Chem. B* 2010; **114**: 14298–14302.
15. Johansson E, Hurley PT, Brunschwig BS and Lewis NS. *J. Phys. Chem. B* 2009; **113**: 15239–15245.
16. Auwärter W, Écija D, Klappenberger F and Barth JV. *Nat. Chem.* 2015; **7**: 105–110.
17. Morris AJ, Meyer GJ and Fujita E. *Acc. Chem. Res.* 2009; **42**: 1983–1994.
18. Maurin A and Robert M. *J. Am. Chem. Soc*. 2016; **138**: 2492–2495.
19. Lin S, Diercks CS, Zhang YB, Kornienko N, Nichols EM, Zhao Y, Paris AR, Kim D, Yang P, Yaghi OM and Chang CJ. *Science* 2015; **349**: 1208–1213.
20. Swierk JR, Méndez-Hernández DD, McCool NS, Liddell P, Terazono Y, Pahk I, Tomlin JJ, Oster NV, Moore TA, Moore AL, Gust D and Mallouk TE. *Proc. Natl. Acad. Sci. USA*. 2015; **112**: 1681–1686.
21. Sommer DJ, Vaughn MD and Ghirlanda G. *Chem. Commun*. 2014; **50**: 15852–16001.
22. Lindsey JS and Bocian DF. *Acc. Chem. Res*. 2011; **44**: 638–650.
23. Savéant J-M. *Chem. Rev.* 2008; **108**: 2348–2378.
24. Civic MR and Dinolfo PH. *ACS Appl. Mater. Interfaces* 2016; **8**: 20465–20473.
25. Kumar B, Llorente M, Froehlich J, Dang T, Sathrum A and Kubiak CP. *Annu. Rev. Phys. Chem.* 2012; **63**: 541–569.
26. Ardo S, Achey D, Morris AJ, Abrahamsson M and Meyer GJ. *J. Am. Chem. Soc.* 2011; **133**: 16572–16580.
27. Walter MG, Rudine AB and Wamser CC. *J. Porphyrins Phthalocyanines* 2010; **14**: 759–792.
28. Dogutan DK, Kwabena Bediako D, Graham DJ, Lemon CM and Nocera DG. *J. Porphyrins Phthalocyanines* 2015; **19**: 1–8.
29. Manbeck GF and Fujita E. *J. Porphyrins Phthalocyanines* 2015; **19**: 46–64.
30. Behar D, Dhanasekaran T, Neta P, Hosten CM, Ejeh D, Hambright P and Fujita E. *J. Phys. Chem. A* 1998; **102**: 2870–2877.
31. Dhanasekaran T, Grodkowski J, Neta P, Hambright P and Fujita E. *J. Phys. Chem. A* 1999; **103**: 7742–7748.
32. Halmann M. *Nature* 1978; **275**: 115–116.
33. Grätzel M. *Nature* 2001; **414**: 338–344.
34. Standing A, Assali S, Gao L, Verheijen MA, van Dam D, Cui Y, Notten PHL, Haverkort JEM and Bakkers EPAM. *Nat. Commun.* 2015; **6**: 7824.
35. Sun J, Liu C and Yang P. *J. Am. Chem. Soc.* 2011; **133**: 19306–19309.
36. Liu C, Sun J, Tang J and Yang P. *Nano Lett.* 2012; **12**: 5407–5411.
37. Khusnutdinova D, Flores M, Beiler AM and Moore GF. *Photosynthetica* 2018; **56**: 67–74.
38. Khusnutdinova D, Beiler AM, Wadsworth BL, Jacob SI and Moore GF. *Chem. Sci.* 2017; **8**: 253–259.
39. Chizhova NV, Kumeev RS and Mamardashvili NZh. *Russ. J. Inorg. Chem.* 2013; **56**: 740–743.
40. Beiler AM, Khusnutdinova D, Jacob SI and Moore GF. *ACS Appl. Mater. Interfaces* 2016; **8**: 10038–10047.
41. Beiler AM, Khusnutdinova D, Jacob SI and Moore GF. *Ind. Eng. Chem. Res.* 2016; **55**: 5306–5314.
42. Beiler AM, Khusnutdinova D, Wadsworth BL and Moore GF. *Inorg. Chem.* 2017; **56**: 12178–12185.
43. Krawicz A, Yang J, Anzenberg E, Yano J, Sharp ID and Moore GF. *J. Am. Chem. Soc.* 2013; **135**: 11861–11868.
44. Cedeno D, Krawicz A, Doak P, Yu M, Neaton J and Moore GF. *J. Phys. Chem. Lett.* 2014; **5**: 3222–3226.
45. Cedeno D, Krawicz A and Moore GF. *Interface Focus* 2015; **5**: 20140085/1–20140085/6.
46. Lummerstorfer T and Hoffmann H. *Langmuir* 2004; **20**: 6542–6545.
47. Lummerstorfer T and Hoffmann H. *J. Phys. Chem. B* 2004; **108**: 3963–3966.
48. Lummerstorfer T, Kattner J and Hoffmann H. *Anal. Bioanal. Chem.* 2007; **388**: 55–64.
49. Wadsworth BL, Beiler AM, Khusnutdinova D, Jacob SI and Moore GF. *ACS Catal.* 2016; **6**: 8048–8057.
50. Allara D and Stapleton J. In Optical Techniques, *Springer Series in Surface Science,* Vol. 51 2013, pp. 59–98.

51. Zhang Z, Hou S, Zhu Z and Liu Z. *Langmuir* 2000; **16**: 537–540.
52. Şen P, Hirel C, Andraud C, Aronica C, Bretonnière Y, Mohammed A, Ågren H, Minaev B, Minaeva V, Baryshnikov G, Lee H-H, Duboisset J and Lindgren M. *Materials* 2010; **3**: 4446–4475.
53. Alben JO, Choi SS, Adler AD and Caughey WS. *Ann. NY. Acad. Sci.* 1973; **206**: 278–295.
54. Li X-Y, Czernuszewicz RS, Kincaid JR and Spiro TG. *J. Am. Chem. Soc.* 1989; **111**: 7012–7023.
55. Nazeeruddin MK, Humphry-Baker R, Officer DL, Campbell WM, Burrell AK and Grätzel M. *Langmuir* 2004; **20**: 6514–6517.
56. Zhang Y-H, Chen D-M, He T and Liu F-C. *Spectrochimica Acta Part A* 2003; **59**: 87–101.
57. Thomas DW and Martell A. *J. Am. Chem. Soc.* 1958; **81**: 5111–5119.
58. Rush III TS, Kozlowski PM, Piffat CA, Kumble R, Zgierski M and Spiro TG. *J. Phys. Chem. B* 2000; **104**: 5020–5034.
59. Nguyen KA, Day PN and Pachter R. *J. Chem. Phys.* 1999; **110**: 9135–9144.
60. Slota R, Broda MA, Dyrda G, Ejsmont K and Mele G. *Molecules* 2011; **16**: 9957–9971.
61. Sun H, Smirnov VV and DiMagno SG. *Inorg. Chem.* 2003; **42**: 6032–6040.
62. Narasimham NA, Nielsen JR and Theimer R. *J. Chem. Phys.* 1957; **27**: 740–745.
63. Panov VP, Kazarin LA, Dubrovin VI and Gusev VV, Kirsh YE. *Zh. Prikl. Spektrosk* 1974; **21**: 862–869.
64. Bar-ilan A and Manassen J. *J. Catal.* 1974; **33**: 68–73.
65. Alben JO, Choi SS, Adler AD and Caughey WS. *Ann. NY. Acad. Sci.* 1973; **206**: 278–295.
66. Boucher LJ and Katz JJ. *J. Am. Chem. Soc.* 1967; **89**: 1340–1345.
67. Kincaid J and Nakamoto K. *J. Inorg. Nucl. Chem.* 1975; **37**: 85–89.
68. Slota R, Broda MA, Dyrda G, Krzysztof E and Giuseppe M. *Molecules* 2011; **16**: 9957–9971.
69. Borod'Ko YG, Vetchinkin SI, Zimont SL, Ivleva IN and Shul'Ga YM. *Chem. Phys. Lett.* 1976; **42**: 264–267.
70. Chuang TJ, Brundle CR and Rice DW. *Surf. Sci.* 1976; **59**: 413–429.
71. Dillard JG, Schenck CV and Koppelman MH. *Clays Clay Miner.* 1983; **31**: 69–72.